Sensors and Actuators A 171 (2011) 252–259

Contents lists available at SciVerse ScienceDirect

Sensors and Actuators A: Physical

journal homepage: www.elsevier.com/locate/sna

Oriented growth of A_2Te_3 (A = Sb, Bi) films and their devices with enhanced thermoelectric performance

Ming Tan [a], Yao Wang [a], Yuan Deng [a,*], Zhiwei Zhang [a], Bingwei Luo [a], Junyou Yang [b,*], Yibin Xu [c]

[a] Beijing Key Laboratory of Special Functional Materials and Film, School of Chemistry and Environment, Beihang University, Beijing 100191, China
[b] Advanced Energy Materials Laboratory, School of Materials Science and Engineering, Huazhong University of Science and Technology, 1037 Luoyu Road, Wuhan 430074, China
[c] Materials Database Station, National Institute for Materials Science, 1-2-1 Sengen, Tsukuba, Ibaraki 305-0047, Japan

ARTICLE INFO

Article history:
Received 24 March 2011
Received in revised form
14 September 2011
Accepted 15 September 2011
Available online 21 September 2011

Keywords:
Thermal evaporation technique
Oriented growth
Thermoelectric devices
Thermoelectric properties

ABSTRACT

Oriented thermoelectric (TE) *p*-Sb_2Te_3 and *n*-Bi_2Te_3 thin films with special nanostructures have been synthesized by a simple vacuum thermal evaporation technique. The composition and microstructure of the films were studied by X-ray diffraction (XRD) and scanning electron microscopy (SEM), presenting a well preferential crystal growth with dense slender columnar grains grown perpendicular to the substrate, and energy dispersive X-ray spectrum (EDX) indicating the compositions distribution in the films. The electric transport properties, i.e., conductivity and Seebeck coefficient, and the thermal transportation of the oriented films show optimized properties. Prototype devices were built up by *p* and *n* elements in series and parallel circuits. The largest output power and cooling could be achieved in Sb_2Te_3 parallel device with P_{max} = 6.51 μW at ΔT = 106 K, and cooling of 4.1 K at 2 V. The 24-pair *p*–*n* couples series device could output maximum voltage of 313 mV at ΔT = 102 K. The power generation and the cooling of the devices show times enhanced TE performances than those consisting of common films. The results proved that introducing nanostructures into films is an effective choice to obtain high-efficient micro TE device.

1. Introduction

The solid state based conversion of heat to electricity, and vice versa, using thermoelectric (TE) materials have many attracting applications, such as waste heat recovery in automobiles or industrial processes, solar thermal energy generation, optoelectronics, body-heat powered biomedical devices, spot cooling of microelectronics, and so on [1–5]. However, the low output power and cooling efficiency have long been the problems of the current TE films devices. The output power and cooling efficiency of a thermoelectric module depend largely on the material's TE properties. The TE efficient is defined by figure-of-merit (ZT), which is expressed as $ZT = (S^2\sigma/\kappa)T$, where S, σ, κ, and T are the Seebeck coefficient, electrical conductivity, thermal conductivity and absolute temperature, respectively. ZT can be improved by introducing nano-scale structures in materials [6]. In this way, the Seebeck coefficient can be increased by means of thermionic emission [7–10], and the thermal conductivity can be significantly reduced through enhanced or modified scattering of phonons by the interfaces of quantum wells (QW) superlattices, surfaces of nanowires (NWs), or the grain boundaries in nanocrystalline materials [11–13]. Research on low-dimensional thermoelectrics systems over the last decade has shown that as the dimensionality of a good thermoelectric material is reduced from bulk to lower dimensionality, there are increasing opportunities to enhance its thermoelectric performance by introducing interfaces which will preferentially scatter phonons relative to electrons and by allowing more independent manipulation of the transport coefficients to control the thermoelectric figure-of-merit. It is well-known that nanowires can help to improve the figure of merit. But single nanowire is limited in fabrication TE devices, while nanopillar array can realize wafer-level processing including lithography and anisotropic etching for improving performances of a wafer-scale TE device as proposed recently [14].

Snyder et al. reported that the device with 126 *n*-type and *p*-type $(Bi, Sb)_2Te_3$ TE elements had been fabricated by an electrochemical deposition method. The device can produce estimated output power (P_{max}) of 1 μW by illumination with a lamp, and an average temperature drop of 2 K at the optimal applied current of 110 mA [15]. Böttner et al. reported that the device containing 12 *n*-Bi_2Te_3 and *p*-$(Bi, Sb)_2Te_3$ TE elements was fabricated by sputtering. The maximum output power P_{max} of 0.67 μW was obtained at a temperature different ΔT of 5 K [16]. Takashiri et al. fabricated Bi–Te alloy thin films by a flash evaporation method. The overall size of the films is 24 mm wide, 22 mm long, 1 mm thick, consisting of 7 *p*–*n* couples. The output voltage V_{op} of 83.3 mV and maximum

* Corresponding authors. Tel.: +86 10 82313482; fax: +86 10 82313482.
E-mail addresses: dengyuan@buaa.edu.cn (Y. Deng), junyou.yang@163.com (J. Yang).

0924-4247/$ – see front matter © 2011 Elsevier B.V. All rights reserved.
doi:10.1016/j.sna.2011.09.020

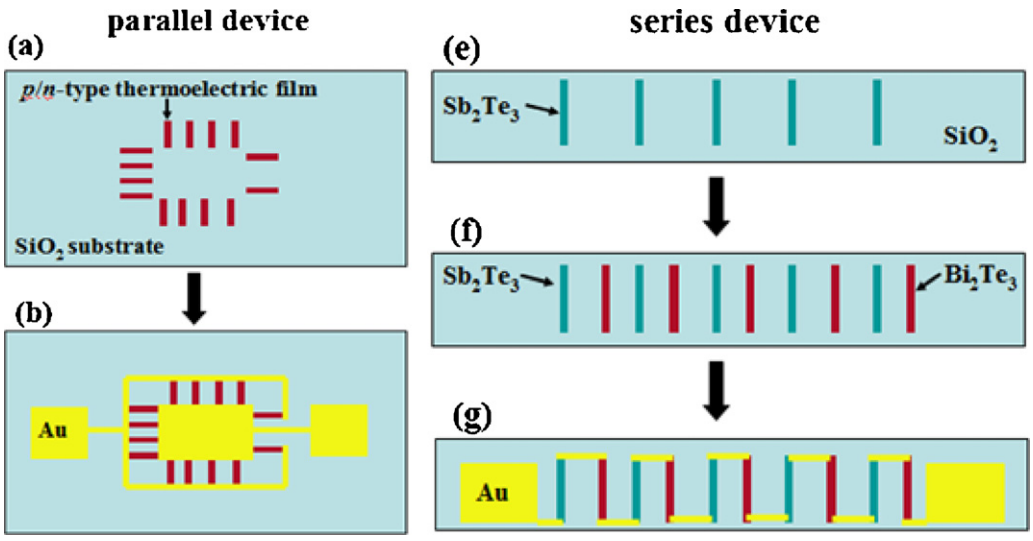

Fig. 1. Process flow of the thermoelectric parallel (left) and series (right) film devices. For the parallel device, (a) First step: p-Sb_2Te_3 or n-Bi_2Te_3 film is deposited by thermal evaporation technique via mask on a glass substrate. (b) Second step: the electrode Au is sputtered onto TE films using mask, then a parallel device is fabricated. For the series device, (e) First step: p-Sb_2Te_3 film is deposited by thermal evaporation technique via mask on a glass substrate. (g) Second step: n-Bi_2Te_3 film is deposited using another mask. (c) Third step: the electrode Au is sputtered onto TE films using mask to electrically connect the p- and n-type elements, then a series device is fabricated.

output power P_{max} of 0.21 μW were obtained at a temperature different ΔT of 30 K [17]. da Silva and Kaviany fabricated a micro TE cooler with 60 pairs of n-type Bi_2Te_3 and p-type Sb_2Te_3 elements using co-evaporation. The thickness and diameter of each columnar element are approximately 4.5 μm and 40 μm, respectively. A maximum temperature different ΔT_{max} of 1.3 K was obtained at an operating current of 23 mA [18].

Recently, based on these nanostructured TE materials, the solid-state power generation and cooling devices have showed high-power energy conversion and a potential to be applied commercially in large-scale. The success of these applications requires the development of a versatile assembly process for producing large area ordered nanostructure. Chowdhury and Venkatasubramanian et al. have made a giant stride forward in enhancing the cooling efficiency of the TE devices by employing nanostructured TE films. A 7×7 array consisting of p-Bi_2Te_3/Sb_2Te_3 and n-$Bi_2Te_3/Bi_2Te_{2.83}Se_{0.17}$ superlattice couples, prepared by metal organic vapor phase deposition, could produce a cooling as much as 15 K at 3 A current [19].

It is still a challenge to find a simple and universal strategy with a high degree of control for fabricating oriented thermoelectric nanostructures. In our previous work, Bi_2Te_3 thin films, composed of ordered nanowire arrays, have been successfully fabricated by a convenient physical vapor deposition method without using any template [20]. Here, we grow density p-Sb_2Te_3 and n-Bi_2Te_3 films with ordered slender columns nanostructures by a simple thermal evaporation method. Continuously, compactly and orderly p-Sb_2Te_3 or n-Bi_2Te_3 thin films can grow on a substrate in a large scale. By using masks, different patterns of TE micro devices were constructed by these films as elements. Then, enhanced thermoelectric performance was obtained.

2. Experimental

The p-Sb_2Te_3 and n-Bi_2Te_3 films were successfully grown on SiO_2 substrate by the thermal evaporation technique. Sb_2Te_3 and Bi_2Te_3 powder (99.99% in purity) were mounted onto the evaporating dish, and the evaporated currents were 165 A and 160 A for ordered Sb_2Te_3 and Bi_2Te_3 films, respectively. While morphologically disordered Sb_2Te_3 and Bi_2Te_3 films were produced for 155 A and 150 A, respectively. Before deposition, the substrates were first cleaned by diluted nitric acid, and then acetone, and dried under the nitrogen airflow. The working pressure was maintained at 2×10^{-6} Torr in the deposition process for all the films.

Two sets of stainless steel masks were prepared to fabricate different electrically connected devices, i.e., in parallel or in series, and each set of masks contain mask for TE films ($mask_f$) and mask for electrode ($mask_e$), respectively. Fig. 1 shows the process flow of the thermoelectric devices obtained using a simple vacuum thermal evaporation technology. Illustrations of the process sequence and schematics of the fabricated thermoelectric devices are presented. The size of parallel device is 22 mm × 10 mm with each TE element 2.5 mm × 0.2 mm in area. Sb_2Te_3 (or Bi_2Te_3) film was first deposited onto substrate under $mask_f$, and then Au electrode was sputtered onto TE films using $mask_e$. Thus, a parallel device consisting of 38 elements of p-type Sb_2Te_3 (or n-type Bi_2Te_3) was produced. For the series device, the total size is 30 mm × 4 mm with each TE element 3 mm × 0.2 mm in area. 24 p-Sb_2Te_3 and n-Bi_2Te_3 elements were separately deposited under $mask_f$, and then Au was sputtered using $mask_e$ to electrically connect the p- and n-type elements. This geometry allows us to obtain a series device consisting of 24 p-n couples with Sb_2Te_3 and Bi_2Te_3 arranged in alternation. The total thickness of all the TE films is 3 μm and the electrode thickness is 400 nm.

The crystal structure of the films was examined by X-ray diffraction (XRD, Rigaku D/MAX 2200) with Cu Ka radiation (λ = 0.154056 nm). The morphology of the films was observed by field emission scanning electron microscopy (FE-SEM, Sirion 200). Electrical conductivity and Seebeck coefficient of the films were examined by ZEM-3 (Ulvac Riko, Inc.) with a self-made test holder for film measurement in the plane direction within the accuracies of 4%. The out-plane thermal conductivity data was collected using TCN-2ω (Omega) (Ulvac Riko, Inc.) at the room temperature. We measured the thermal resistance of the films with different thicknesses at different frequencies (400, 500, 1000 and 1500 Hz) and calculated the slope of the curve about thermal resistance of the films with different thicknesses. Thus, the thermal conductivity of the film (κ_f) is calculated as below:

$$\kappa_f = \frac{1}{S_c + ((D_f \cdot S_f)/(\kappa_g \cdot D_g \cdot S_g))}$$

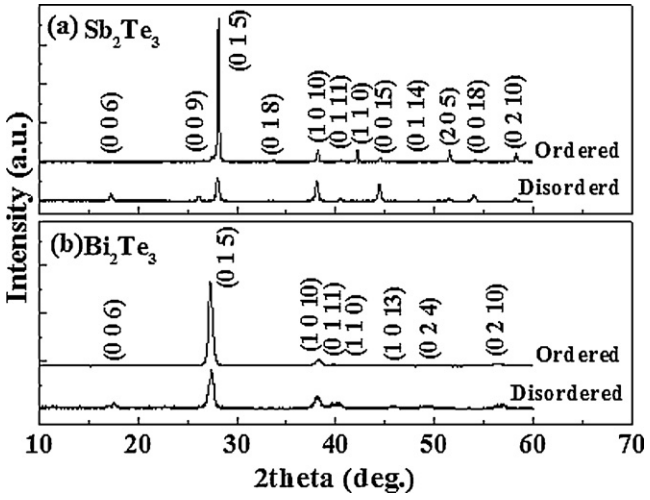

Fig. 2. XRD patterns of (a) Sb_2Te_3 and (b) Bi_2Te_3 films.

where S_c is a slope of the curve about thermal resistance versus thickness of the films, D_f is density of the thin film, S_f is specific heat of the thin film, and κ_g, D_g, S_g are thermal conductivity, density, specific heat of the glass substrate, respectively. A four-probe method with Hall effect measurement (ECOPIA HMS-3000) was employed to determine the concentration (n) and mobility (μ) of the carriers through the equations $n = \gamma A/eR_H$ and $\mu = R_H/\rho$, respectively, where R_H is Hall coefficient, γ is the structure factor, A is the Hall factor, e is the electron charge, and ρ is the electrical resistivity. We have also measured the overall resistance of the thin thermoelectric devices by voltammetry. The output voltages of the devices were measured by DC digital voltage/current meter (Shanghai SB-2238) when supplying a temperature difference between hot and cold sides of the devices.

3. Results and discussion

Oriented p-Sb_2Te_3 and n-Bi_2Te_3 thin films with special nanostructure have been synthesized by a simple vacuum thermal evaporation technique, which show a preferential growth in the films. XRD patterns of Sb_2Te_3 and Bi_2Te_3 films were shown in Fig. 2. For the Sb_2Te_3 films, all peaks are indexed as rhombohedral phase (JCPDS 71-0393) (shown in Fig. 2a). The intensity of (0 1 5) peak of Sb_2Te_3 is dramatically strong as compared with standard card, indicating a highly preferential orientation of the Sb_2Te_3 film along the (0 1 5) directions. Shown in Fig. 2b, the diffraction patterns of Bi_2Te_3 film match the rhombohedral structure (JCPDS 15-0863). Different from Sb_2Te_3 film, Bi_2Te_3 film shows only few major diffraction peaks. The intensity of (0 1 5) peak is also dramatically strong, and other peaks became weak or even disappear, indicating highly preferential growth along [0 1 5] orientation.

The microstructures of p-Sb_2Te_3 and n-Bi_2Te_3 thin films were shown in Fig. 3. Seen from the top view (shown in Fig. 3a and e), the films are dense and uniform. Besides, many small grains distribute on the Bi_2Te_3 film surface in Fig. 3e. The high density of small grains is benefit for enhancing the properties of TE films. Seen from the cross-sectional images of the films (Fig. 3b and f), Sb_2Te_3 and Bi_2Te_3 grains were grown in well ordered slender columnar shape perpendicular to the substrates, along their preferential growth directions. The diameters of the columnar grains are estimated to be 10–100 nm for the ordered Sb_2Te_3 film and Bi_2Te_3 film. By changing the deposition time in our experiment, the thickness of films can be controlled to be above 5 μm. EDX analysis shows slightly Sb or Bi composition segregation in the films (see Table 1). The formation energy for vacancies or antisite defects (Sb or Bi on the Te sublattice) is low in Sb_2Te_3 or Bi_2Te_3. These excess Sb or Bi atoms can be in the form of Sb or Bi antisite atoms, that is, Sb or Bi replaces Te creating a carrier, which contribute to the increase in electrical conductivity.

The guiding principle in vapor phase growth is to control the supersaturation of the vapors. The degree of supersaturation plays an important role in the control over the morphology of the obtained nanostructures. Generally, high supersaturation leads to the growth of small powders, while medium supersaturation is favorable for the preparation of whisker and nanowires, and low supersaturation for bulk crystal growth. In our experiment, the degree of supersaturation is controlled by the evaporated currents.

By controlling growth parameter, the films microstructures have changed obviously as shown in Fig. 3. When the evaporated current is lower, the disordered Sb_2Te_3 or Bi_2Te_3 film is obtained, which is obviously disordered stacked by hexagonal plates (shown in Fig. 3g and h). The sizes of the grains are estimated to be 30–200 nm for the disordered Sb_2Te_3 and Bi_2Te_3 films. The intensity of (0 1 5) peak of the above disordered Sb_2Te_3 film is weak (shown in Fig. 2a), which indicates that the preferential growth of (0 1 5) direction is the essential reason for the formation of oriented columnar. The diffraction patterns of disordered Bi_2Te_3 film well match the rhombohedral structure (JCPDS 15-0863, shown in Fig. 2b).

The effects of morphology of films on the in-plane electrical conductivity, Seebeck coefficient, and out-plane thermal conductivity were studied as shown in Table 1. Electrical conductivities of the disordered films were obtained at room temperature, with $\sigma_{Sb_2Te_3} = 2.4 \times 10^4$ S/m and $\sigma_{Bi_2Te_3} = 9.12 \times 10^4$ S/m, respectively. While electrical conductivities of the oriented films is $\sigma_{Sb_2Te_3} = 8.05 \times 10^4$ S/m and $\sigma_{Bi_2Te_3} = 12.8 \times 10^4$ S/m, which are higher than those of the prepared disordered films and the reported values of Sb_2Te_3 and Bi_2Te_3 films [18,21]. The ordered microstructures of TE films composed of nano-sized columnar grains should be responsible for high electrical conductivity. Perhaps the compact microstructure is benefit for enhancing the mobility of carriers, this is, the strong orientation plane constitutes a relatively preferential way for carriers transport and promotes the carriers mobility and electrical conductivity. The Seebeck coefficients (S) are measured to be about 164 μV K^{-1} and −85 μV K^{-1} for the oriented Sb_2Te_3 and Bi_2Te_3 films at RT, respectively, while $S_{Sb_2Te_3} = 132$ μV K^{-1} and $S_{Bi_2Te_3} = -46$ μV K^{-1} for the disordered Sb_2Te_3 and Bi_2Te_3 films. Then as-prepared Sb_2Te_3 film is a p-type semiconductor and Bi_2Te_3

Table 1
Transport properties and compositions of thin films measured at room temperature.

Films	Carrier concentration[a] (10^{20}/cm^3)	Carrier mobility[a] (cm^2/(V s))	Electrical conductivity[b] (10^4 S/m)	Seebeck coefficient (μV/K)	Thermal conductivity (W/(m K))	Sb or Bi/Te atomic ratio
Ordered Sb_2Te_3	4.4	81	8.05	164	0.78	41.2/58.8
Disordered Sb_2Te_3	4.9	31	2.4	132	–	41.4/58.6
Ordered Bi_2Te_3	−57	75	12.8	−85	0.91	42/58
Disordered Bi_2Te_3	−6.8	23	9.12	−46	–	41.7/58.3

[a] The data are determined by ECOPIA HMS-3000.
[b] The data are directly measured by ZEM.

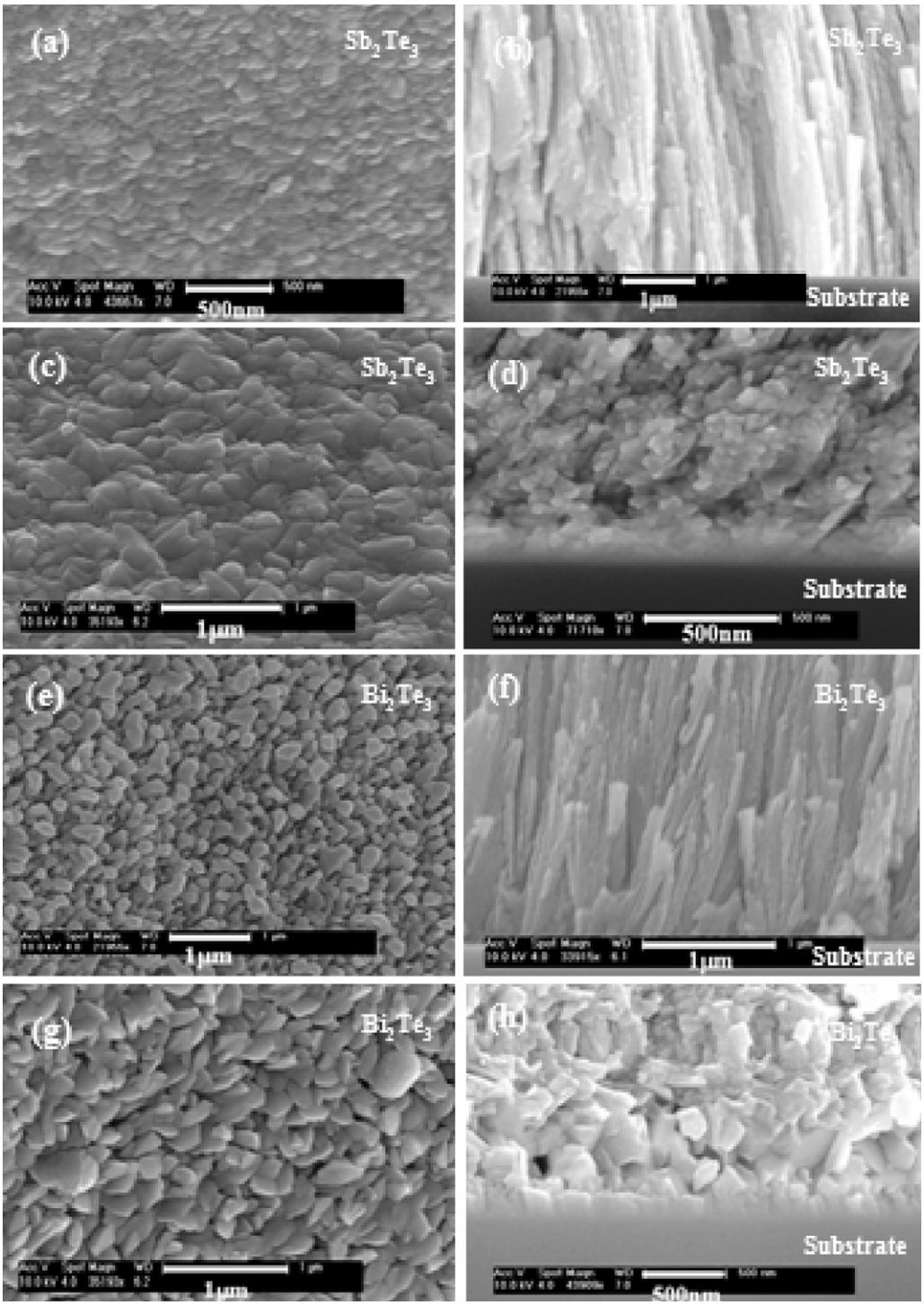

Fig. 3. SEM images of (a, b) oriented and (c, d) disoriented Sb_2Te_3 films with (a, c) top-view and (b, d) cross-sectional view, respectively; SEM images of (e, f) oriented and (g, h) disoriented Bi_2Te_3 films with (e, g) top-view and (f, h) cross-sectional view, respectively.

film is *n*-type one. The Seebeck coefficient and electrical conductivity in the films with oriented column arrays are promisingly higher than those of disordered films, which also indicate the oriented nanostructures are beneficial to the improving thermoelectric performance. The out of plane thermal conductivity of the oriented Sb_2Te_3 and Bi_2Te_3 are 0.78 W/(m K) and 0.91 W/(m K), respectively, which are lower than that reported for Sb_2Te_3 and Bi_2Te_3 materials [22–26]. The lattice thermal conductivity, κ_{latt} (according the Wiedemann–Franz law $\kappa_{latt} = \kappa - L\sigma T$ with a Lorentz number $L = 1.3 \times 10^{-8}\,W\,\Omega\,K^{-2}$ which indicates a significant reduction in the Lorenz factor compared with $2.44 \times 10^{-8}\,W\,\Omega\,K^{-2}$, owing to non-parabolicity of the bands and various scattering mechanisms are taken into consideration in non-degenerate Bi_2Te_3-based semiconductors with low dimensional structure [12,26–28]), are about $0.47\,W\,m^{-1}\,K^{-1}$ and $0.41\,W\,m^{-1}\,K^{-1}$ for the ordered Sb_2Te_3 and Bi_2Te_3 films, respectively, which are much less than the reported values of the films [26]. Thermal conductivity of the ordered Sb_2Te_3 and Bi_2Te_3 are lower than that of the materials as expected because of its unique build-up structures. It is explained that a large number of nanoscaled grains effectively scatter phonons over a

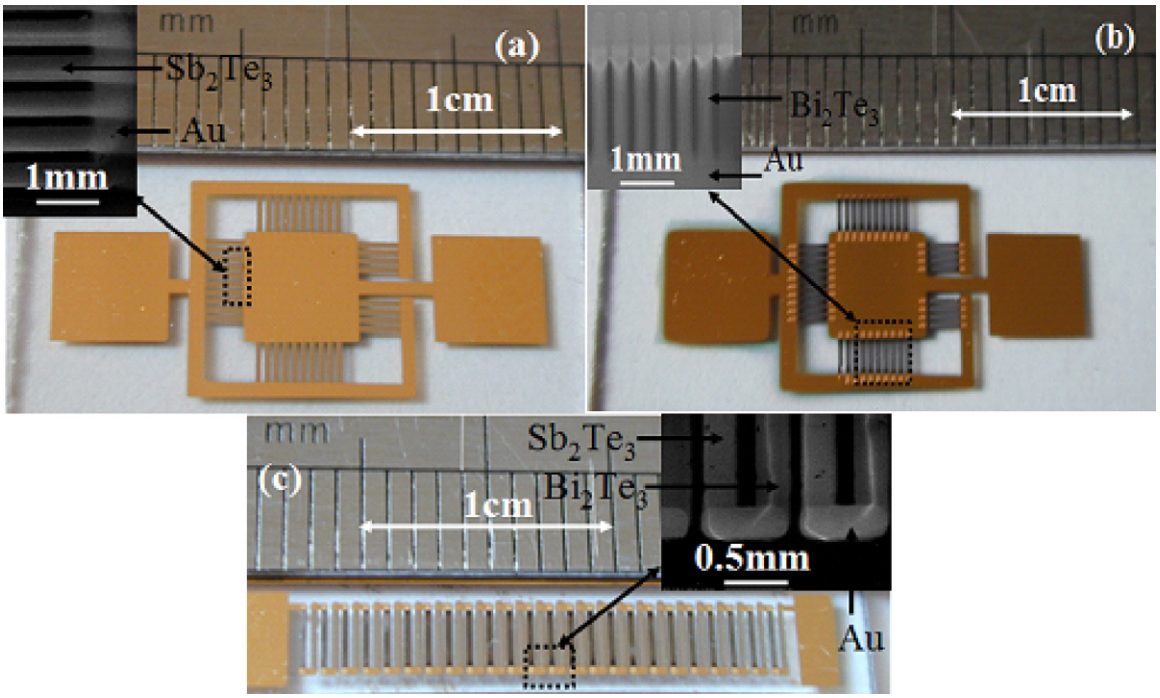

Fig. 4. Photographs of (a) Sb_2Te_3, (b) Bi_2Te_3, (c) Bi_2Te_3–Sb_2Te_3 devices and the insets show the SEM images electrode/TE films interconnects.

wide range of frequencies as long as it has sufficiently small grain size. Besides, there will be increased phonon scattering from the grains boundaries or the interfaces of the ordered slender columnar-shape grains. If the thermal conductivities of the two films were nearly isotropic, ZT of the oriented p-Sb_2Te_3 and n-Bi_2Te_3 films could be estimated to be about 0.83 and 0.3 at RT, respectively. Compared with previous reports on the films prepared by co-evaporation [29], our Sb_2Te_3 film with controlled microstructure shows an improved ZT. However, the ZT of the Bi_2Te_3 film is still low.

To better understand the transport properties of the TE films, Hall effects measurement was carried out at room temperature to study the concentration and mobility of the carriers. It can be seen that the Hall mobility and carrier concentration exhibit greatly different between the oriented nanostructures and the disordered microstructures in Table 1. The films with oriented structures have high mobility of 81 and 75 $cm^2/(V\,s)$ for Sb_2Te_3 and Bi_2Te_3 films, respectively. It may be due to the fact that the compact column arrays are somewhat advantageous to the carrier transport, i.e., the ordered grains interfaces or boundaries contribute to the enhanced carrier mobility. The high values of carrier concentration of the films lead to its relatively high electrical conductivity due to formation lots of defects. Especially in the ordered Bi_2Te_3 film, the column arrays composed of a large number of small grains trap the holes and produce more electrons in the ordered interfaces/boundaries and defects as a result of high carrier concentration. The electrical conductivity of the films is estimated by according to $\sigma = ne\mu$, which are higher than the results measured by ZEM-3. But the high carrier concentration of the films may result in a high thermal conductivity, possibly reducing the figure of merit in the films. Moreover it was also observed that the disordered films have a lower mobility than the oriented films. Two possible explanations are, firstly, more disordered grain boundaries scatter charge carriers in the disoriented thin films, and secondly the collisions of charge carriers with each other become significant when carrier concentration is higher in the films.

Subsequently, TE devices were constructed using these disordered or oriented p-Sb_2Te_3 and n-Bi_2Te_3 films. Two types of circuit were designed, one is electrically connected in parallel, and the other is in series. Fig. 4 shows photographs of devices constituted by oriented p-Sb_2Te_3 or n-Bi_2Te_3 elements in parallel, respectively, and p-Sb_2Te_3/n-Bi_2Te_3 film elements in series. The insets in Fig. 4 further show detailed morphology of the electrode/TE films interconnect to make sure they are in good electrical contact, which is a key issue in guaranteeing device performance.

The resistances of the morphologically disordered p-Sb_2Te_3, n-Bi_2Te_3 and p-Sb_2Te_3/n-Bi_2Te_3 films devices are 7.8 Ω, 6.5 Ω and 8.1 kΩ, respectively. While by introducing the oriented nanostructure into the films, the resistances approach to 6.9 Ω, 4.7 Ω and 7.2 kΩ correspondingly (see Table 2). The resistances are still relatively high due to relatively high resistance of the TE films and the contact resistance between electrode and TE films. The columnar grains with the size of tens nanometers form large number of grain boundaries perpendicular to the substrate, which will contribute to the increase of film in-plane resistance. On the other hand, these boundaries might be benefit for the reduction of in-plane lattice thermal conductivity due to the increase of phonon scattering at interfaces. Some electrode/TE film interface is clear and has sharp edge (see the inset in Fig. 4c), but sometimes, the interface is vague with two materials mutually diffusing (see the inset in Fig. 4b). Thus there is a great room for decreasing of resistance by the improvement of TE device construction processing to lower the contact resistance. The contact resistance is expected to be reduced using an interface layer between metallic junctions and thermoelectric elements, and annealed process. Besides, the thickness of electrode is thinner than its TE films. The electrodes may possibly break by thermal shock, leading to the high electrical resistivity in the devices fabrication process.

The performance of these devices as power generator and cooler has been valued. To measure the open output voltage under a temperature difference (ΔT), we heated one side of the TE element and cooled the other side by using a specific accessory. The maximum output power was estimated by the open output voltage and internal resistance of device. Fig. 5 shows the variation of open output voltage (V_{op}, squares) and output power (P, circles) with temperature difference of devices. For each device, the V_{op} increases

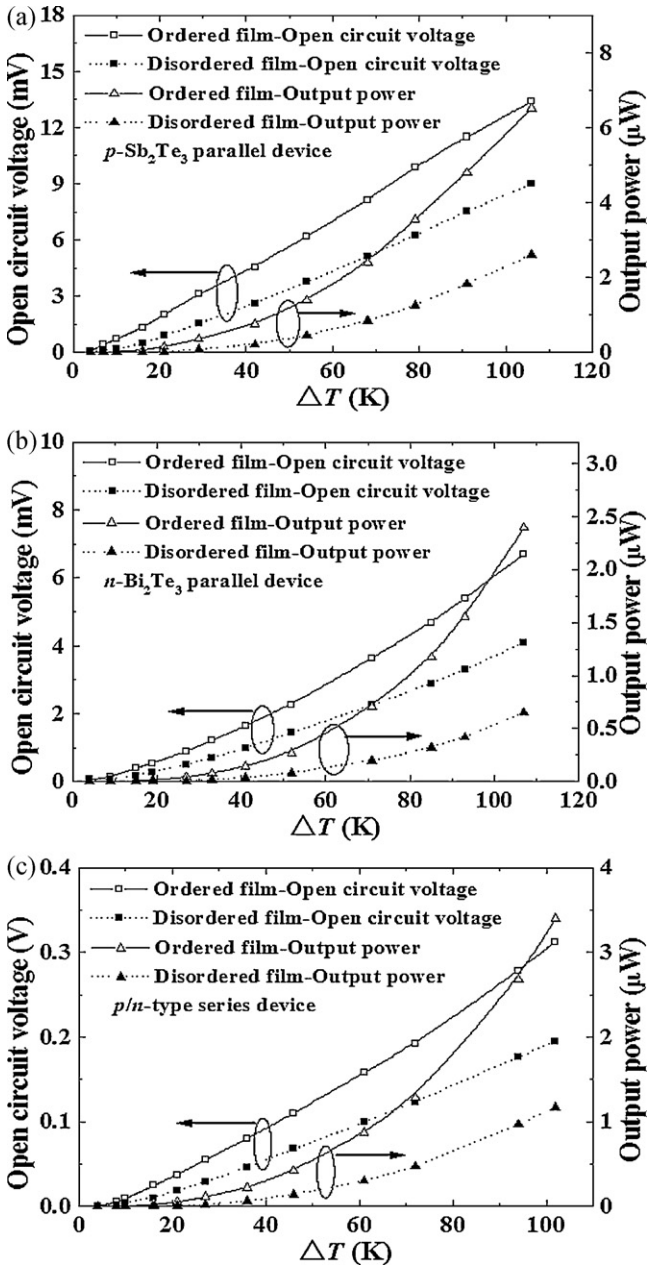

Fig. 5. Open output voltage (square) and output power (triangle) change with temperature difference of the (a) p-Sb_2Te_3 parallel device, (b) n-Bi_2Te_3 parallel device and (c) p-Sb_2Te_3/n-Bi_2Te_3 series device.

approximately linearly with temperature difference, which also implies that the S nearly remains constant with temperature. In contrast to the bulk Sb_2Te_3 and Bi_2Te_3 materials, whose Seebeck coefficients decrease as the temperature increases, the temperature stability of S of the oriented p-Sb_2Te_3 and n-Bi_2Te_3 films are useful when the TE device is in practical use.

The measured output voltage was lower than the expected voltage calculated from the Seebeck coefficient of the thin films, especially for the series device with 24 p–n couples. This may come from the electric loss at the interconnects because of the contact resistance, and measurement error on the exact temperature at hot side. P_{max} is proportional approximately to $(\Delta T)^2$ because $P_{max} = {V_{op}}^2/4R_{in}$, where R_{in} is the internal resistance of a device ($R_{in} = R_n + R_p + R_c + R_l$, R_n and R_p are the electrical resistances of n-type and p-type thermoelements, respectively; R_c is the total electrical contact resistance; R_l is the total electrical interconnect resistance).

The highest values of V_{op} and P_{max} for these devices as power generator are summarized in Table 2. In these devices with the disordered films, for the 38 p-type Sb_2Te_3 parallel device, V_{op} is 9 mV and P_{max} is 2.6 μW at ΔT = 106 K. V_{op} of the n-type Bi_2Te_3 parallel device is 4.1 mV and P_{max} is 0.65 μW at ΔT = 107 K; and V_{op} of 24-pair p-Sb_2Te_3/n-Bi_2Te_3 couples series device is 195 mV and P_{max} is 1.17 μW at ΔT = 102 K. While the power performances of such devices are greatly enhanced when introducing the oriented nanostructure into the films. V_{op} and P_{max} of 38 p-type Sb_2Te_3 parallel device are up to 13.4 mV and 6.51 μW at ΔT = 106 K, respectively; V_{op} and P_{max} of the n-type Bi_2Te_3 parallel device are enhanced to 6.7 mV and 2.39 μW at ΔT = 107 K; and for 24-pair p-Sb_2Te_3/n-Bi_2Te_3 couples series device, V_{op} = 313 mV and P_{max} = 3.4 μW are obtained at ΔT = 102 K. p-type Sb_2Te_3 parallel device shows the highest output power due to larger absolute value of S_p. Though V_{op} of 24-pair series device is multiplied than that of parallel device, the P_{max} is lower than expected, which may come from big difference in Seebeck coefficient absolute values between the p- and n-type materials, and relatively larger contact resistance in the series pattern. Compared with reported performances of TE film devices, e.g., P_{max} = 23.3 nW of 60-pair device at ΔT = 160 K, and P_{max} = 65 nW of 120-pair device at ΔT = 168 K [30], and V_{op} = 83.3 mV and estimated P_{max} = 0.21 μW obtained from 7 p–n bismuth–telluride alloy thin film generators at ΔT = 30 K [17], the devices with oriented nanostructure show excellent performance. This implies our TE film devices with high relatively intrinsic ZT values can efficiently convert heat into electricity. At the same time, the geometry configuration of devices and processing technique are greatly sophisticated and effective in our experiments. By simple calculation, we could know that when contact resistance was decreased by half, the highest output power could be increased about 8–17% for the devices. To be specific, if R_c of the ordered n-type Bi_2Te_3 device was reduced to 0.7 Ω, assuming V_{op} = 6.7 mV, the output power will be 2.8 μW at ΔT = 107 K, then the highest output power could be increased about 17%.

On the other hand, the cooling of these devices has been also measured. Among the disordered films devices, p-type Sb_2Te_3 and n-type Bi_2Te_3 parallel devices produced ΔT = 3.1 K and 2.2 K at 2 V work voltage, respectively. Only $\Delta T \approx 1$ K was obtained in 24 pair p–n couples series device at 5 mA current. But ΔT = 4.1 K, 2.9 K, and 1.4 K were achieved for the oriented p-type, n-type, and p-n type films devices, respectively, under the same work conditions. A factor that should be considered in microcoolers is the heat conduction from the metal wire to the cold side of the devices. This will reduce the maximum cooling. In addition, the thermal resistance of the

Table 2
The highest open output voltage (V_{op}) and output power (P_{max}) as a function of temperature difference of the six set of devices.

Types	Devices	R_{in} (Ω)	R_c (Ω)	ΔT (K)	V_{op} (mV)	P_{max} (μW)
Parallel	Ordered p-Sb_2Te_3	6.9	1.1	106	13.4	6.51
Parallel	Disordered p-Sb_2Te_3	7.8	1.3	106	9	2.6
Parallel	Ordered n-Bi_2Te_3	4.7	1.4	107	6.7	2.39
Parallel	Disordered n-Bi_2Te_3	6.5	1.6	107	4.1	0.65
Series	Ordered p/n-type	7200	1900	102	313	3.4
Series	Disordered p/n-type	8100	2200	102	195	1.17

Table 3
The power factor of the thin films and the cooling performance of the devices.

Films	Devices	$S^2\sigma$ (mW/(m K^2))	V or I	ΔT (K)	Reference
p-Sb_2Te_3	38 p-type	2.17	2 V	4.1	Our work
n-Bi_2Te_3	38 n-type	0.92	2 V	2.9	
p-Sb_2Te_3/n-Bi_2Te_3	24 pair p/n	2.17/0.92	5 mA	1.4	
p-Sb_2Te_3/n-Bi_2Te_3	126 pair p/n	–	110 mA	2	[15]
p-Sb_2Te_3/n-Bi_2Te_3	60 pair p/n	0.3/0.15	23 mA	1.3	[18]
p-Sb_2Te_3/n-Bi_2Te_3	200 pair p/n	0.08/0.3	200 mA	1.2	[21]
p-Sb_2Te_3/n-Bi_2Te_3	1 pair p/n	0.82/3.1	55 mA	15.5	[31]

substrate, the cooling power loss from the side contact, and the Joule heating affect the work performance. It is also very important for the designed sizes of devices due to affecting the maximum cooling. But it further implies that the cooling efficiency of the devices was enhanced obviously through using the films with oriented nanostructure. In contrast with previous results [15,18,21], the cooling of our devices also exhibits improved performance (see Table 3). It indicates that the properties of thermoelectric thin films and the number of couples and the sizes of devices are relatively desired in our work. We expect further optimization in both film materials and the device processing technique, which will yield higher output voltage and power.

4. Conclusions

Oriented p-Sb_2Te_3 and n-Bi_2Te_3 thin films with special nanostructures have been synthesized by a simple vacuum thermal evaporation technique. The films consist of dense slender columnar grains with preferential orientations perpendicular to the substrates. These nanostructured Sb_2Te_3 and Bi_2Te_3 elements were integrated into the devices electrically connected in parallel or in series. Compared with TE devices without oriented TE films, the power generation and cooling performances of the devices were greatly enhanced by introducing oriented films. The largest output power and cooling could be achieved in Sb_2Te_3 parallel device with P_{max} = 6.51 μW at ΔT = 106 K, and cooling of 4.1 K at 2 V. The 24-pair p–n couples series device could output maximum voltage 313 mV at ΔT = 102 K. The results proved that designing TE devices using low-dimensional TE materials with nanostructures is an effective choice to obtain high-efficient micro TE device.

Acknowledgements

The work was supported by National Natural Science Foundation of China under Grant No. 50772005, the National High Technology Research and Development Program of China under Grant No. 2009AA03Z322, Beijing Technology Topic Program under Grant No. Z08000303220808 and Key Laboratory of Photochemical Conversion and Optoelectronic Materials, TIPC, CAS.

References

[1] P. Pichanusakorn, P.R. Bandaru, Minimum length scales for enhancement of the power factor in thermoelectric nanostructures, J. Appl. Phys. 107 (2010), 074304-1-4.
[2] L.E. Bell, Cooling, heating, generating power, and recovering waste heat with thermoelectric systems, Science 321 (2008) 1457–1461.
[3] R. Singh, Z.X. Bian, A. Shakouri, Direct measurement of thin-film thermoelectric figure of merit, Appl. Phys. Lett. 94 (2009), 212508-1-3.
[4] G.S. Wang, Y. Deng, Y. Xiang, L. Guo, Fabrication of radial ZnO nanowire clusters and their PVDF/ZnO composites exhibit enhanced dielectric properties, Adv. Funct. Mater. 18 (2008) 584–588.
[5] A. Majumdar, Thermoelectric devices: helping chips to keep their cool, Nat. Nanotechnol. 4 (2009) 214–215.
[6] L.D. Hicks, M.S. Dresselhaus, Effect of quantum-well structures on the thermoelectric figure of merit, Phys. Rev. B 47 (1993) 12727–12731.
[7] G. Zeng, J.M.O. Zide, W. Kim, J.E. Bowers, A.C. Gossard, Z. Bian, Y. Zhang, A. Shakouri, S.L. Singer, A. Majumdar, Cross-plane Seebeck coefficient of ErAs:InGaAs/InGaAlAs superlattices, J. Appl. Phys. 101 (2007), 034502-1-5.
[8] A. Shakouri, J.E. Bowers, Heterostructure integrated thermionic coolers, Appl. Phys. Lett. 71 (1997) 1234–1236.
[9] D. Vashaee, A. Shakouri, Improved thermoelectric power factor in metal-based superlattices, Phys. Rev. Lett. 92 (2004), 106103-1-4.
[10] T. Thonhauser, T.J. Scheidemante, J.O. Sofo, J.V. Badding, G.D. Mahan, Thermoelectric properties of Sb_2Te_3 under pressure and uniaxial stress, Phys. Rev. B 68 (2003), 085201-1-8.
[11] A.I. Boukai, Y. Bunimovich, J. Tahir-Kheli, J.K. Yu, W.A. Goddard III, J.R. Heath, Silicon nanowires as efficient thermoelectric materials, Nature 451 (2008) 168–171.
[12] R. Venkatasubramanian, E. Siivola, T. Colpitts, B. O'Quinn, Thin-film thermoelectric devices with high room-temperature figures of merit, Nature 413 (2001) 597–602.
[13] B. Poudel, Q. Hao, Y. Ma, Y. Lan, A. Minnich, B. Yu, X. Yan, D. Wang, A. Muto, D. Vashaee, X. Chen, J. Liu, M.S. Dresselhaus, G. Chen, Z.F. Ren, High thermoelectric performance of nanostructured bismuth antimony telluride bulk alloys, Science 320 (2008) 634–638.
[14] A. Stranz, Ü. Sökmen, J. Kähler, A. Waag, E. Peiner, Measurements of thermoelectric properties of silicon pillars, Sens. Actuators A: Phys. 171 (2011) 48–53.
[15] G.J. Snyder, J.R. Lim, C.K. Huang, J.P. Fleurial, Thermoelectric microdevice fabricated by a MEMS-like electrochemical process, Nature 2 (2003) 528–531.
[16] H. Böttner, J. Nurnus, A. Gavrikov, G. Kuhner, M. Jägle, C. Künzel, D. Eberhard, G. Plescher, A. Schubert, K.H. Schlereth, New thermoelectric components using microsystem technologies, J. Microelectromech. Syst. 13 (3) (2004) 414–420.
[17] M. Takashiri, T. Shirakawa, K. Miyazaki, H. Tsukamoto, Fabrication and characterization of bismuth–telluride-based alloy thin film thermoelectric generators by flash evaporation method, Sens. Actuators A 138 (2007) 329–334.
[18] L.W. da Silva, M. Kaviany, Fabrication and measured performance of a first-generation microthermoelectric cooler, J. Micro. Syst. 14 (2005) 1110–1117.
[19] I. Chowdhury, R. Prasher, K. Lofgory, G. Chrysler, S. Narasimhan, R. Mahajan, R. Alley, R. Venkatasubramanian, On-chip cooling by superlattice-based thin-film thermoelectrics, Nat. Nanotechnol. 4 (2009) 235–238.
[20] Y. Deng, Y. Xiang, Y.Z. Song, Template-free synthesis and transport properties of Bi_2Te_3 ordered nanowire arrays via a physical vapor process, Cryst. Growth Des. 9 (2009) 3079–3082.
[21] I.Y. Huang, J.C. Lin, K.D. She, M.C. Li, Development of low-cost micro-thermoelectric coolers utilizing MEMS technology, Sens. Actuators A 148 (2008) 176–185.
[22] O. Yamashita, S. Tomiyoshi, High performance n-type bismuth–telluride with highly stable thermoelectric figure of merit, J. Appl. Phys. 95 (2004) 6277–6283.
[23] S. Wang, W.J. Xie, H. Li, X.F. Tang, High performance n-type $(Bi, Sb)_2(Te, Se)_3$ for low temperature thermoelectric generator, J. Phys. D 43 (2010), 335404-1-8.
[24] Y. Ma, Q. Hao, B. Poudel, Y.C. Lan, B. Yu, D.Z. Wang, G. Chen, Z.F. Ren, Enhanced thermoelectric figure-of-merit in p-type nanostructured bismuth antimony tellurium alloys made from elemental chunks, Nano Lett. 8 (2008) 2580–2584.
[25] A. Datta, J. Paul, A. Kar, A. Patra, Z.L. Sun, L.D. Chen, J. Martin, G. Nolas, Facile chemical synthesis of nanocrystalline thermoelectric alloys based on Bi–Sb–Te–Se, Cryst. Growth Des. 10 (2010) 3983–3989.
[26] N. Peranio, O. Eibl, Structural and thermoelectric properties of epitaxially grown Bi_2Te_3 thin films and superlattices, J. Appl. Phys. 100 (2006), 114306-1-10.
[27] H. Beyer, J. Nurnus, H. Böttner, A. Lambrecht, E. Wagner, G. Bauer, High thermoelectric figure of merit ZT in PbTe and Bi_2Te_3-based superlattices by a reduction of the thermal conductivity, Physica E 13 (2002) 965–968.
[28] C.M. Bhandari, D.M. Rowe, Electronic contribution to the thermal conductivity of narrow band gap semiconductors-effect of non-parabolicity of bands, J. Phys. D: Appl. Phys. 18 (1985) 873–884.
[29] L.M. Goncalves, J.G. Rocha, Application of microsystems technology in the fabrication of thermoelectric micro-converters, in: J.W. Swart (Ed.), Solid State Circuits Technologies, 2010, pp. 385–397.
[30] R. Izaki, N. Kaiwa, M. Hoshino, T. Yaginuma, S. Yamaguchi, Roll-type thermoelectric devices with InN thin films, Appl. Phys. Lett. 87 (2005), 243508-1-3.
[31] H. Zou, D. Rowe, S. Williams, Peltier effect in a co-evaporated Sb_2Te_3(p)–Bi_2Te_3(n) thin film thermocouple, Thin Solid Films 408 (2002) 270–274.

Biographies

Ming Tan received the BS degree in physics from Tianjin Normal University, China, in 2004, and MS degree in materials physics and chemistry in 2009. Since 2009 he is a PhD-student at Beijing University of Aeronautics and Astronautics, China supervised

by Prof. Yuan Deng. He is working on deposition nanostructured thermoelectric films and thermoelectric power generation and cooling micro-devices.

Yao Wang received the BS degree in materials science and engineering from National University of Defense and Technology, China, in 2004, and PhD degree in materials science and engineering from Tsinghua University, China, in 2009. Since 2009, she joined Prof. Yuan Deng's group in school of chemistry and environment in Beihang University as a lecturer. Her recent researches focus on the growth and characterization functional films, and their applications in prototype devices.

Yuan Deng received the BS and PhD degrees in chemistry from Tsinghua University, China, in 1995 and 2000, respectively. During 2001–2002, he worked as postdoc in department of materials science and engineering, Tsinghua University, China.